

Catalysis Science & Technology

Accepted Manuscript



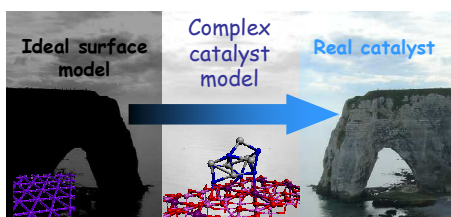
This is an *Accepted Manuscript*, which has been through the Royal Society of Chemistry peer review process and has been accepted for publication.

Accepted Manuscripts are published online shortly after acceptance, before technical editing, formatting and proof reading. Using this free service, authors can make their results available to the community, in citable form, before we publish the edited article. We will replace this *Accepted Manuscript* with the edited and formatted *Advance Article* as soon as it is available.

You can find more information about *Accepted Manuscripts* in the [Information for Authors](#).

Please note that technical editing may introduce minor changes to the text and/or graphics, which may alter content. The journal's standard [Terms & Conditions](#) and the [Ethical guidelines](#) still apply. In no event shall the Royal Society of Chemistry be held responsible for any errors or omissions in this *Accepted Manuscript* or any consequences arising from the use of any information it contains.

Advanced DFT models of complex catalysts, such as amorphous silica-alumina and supported subnanometric platinum particles, bridge the gap between the ideal surface model and the industrial catalyst.



Density Functional Theory simulations
of complex catalytic materials in reactive
environment:
beyond the ideal surface at low coverage

*Céline Chizallet and Pascal Raybaud**

IFP Energies nouvelles, Direction Catalyse et Séparation, Rond-point de l'échangeur de
Solaize, BP3, 69360 Solaize, France

* Corresponding author, Fax: +33 4.37.70.20.66; Tel: +33.4.37.70.23.20 ;

E-mail: pascal.raybaud@ifpen.fr

celine.chizallet@ifpen.fr; pascal.raybaud@ifpen.fr

Abstract.

Most efficient heterogeneous catalysts used industrially are usually very complex systems. Far away from perfect crystallinity and well-defined oriented surfaces at low coverage, they involve structural disorder, heterogeneous sites distribution with variable coordination and structural dependence upon chemical environment. Unravelling their atomic scale structures and understanding their roles in the catalytic reaction are not easy tasks, as the respective contributions of each type of site to the spectroscopic or catalytic responses are generally convoluted. Computational chemistry is of great help to address these issues. In the present perspective review, we highlight two relevant systems involved in numerous industrial applications: amorphous silica alumina support and subnanometric platinum clusters, possibly doped with tin and/or indium, supported on γ -Al₂O₃. The structural complexity is inherent to the amorphous nature of an oxide support on the one hand, and to the ultra-dispersed form of a mono and multi-metallic catalyst, on the other hand. In each case, Density Functional Theory (DFT) calculation was used to provide an original structure for active sites and to reveal how the corresponding multi-steps reactions are influenced. Moreover, we highlight how coverage effects on complex systems, depending on temperature and pressure reaction conditions, offer enriched perspectives beyond those of theoretical studies constrained at the ideal surfaces with low coverage.

Keywords. Amorphous Silica-alumina, platinum, alumina, Density Functional Theory, Pseudo-bridging silanol, Brønsted acid site, reforming, dehydrogenation, cracking

Authors.

Céline Chizallet graduated from Ecole Normale Supérieure (Paris) and Paris 6 University (MSc in 2002). She obtained the "Agrégation de Chimie" in 2003 and a PhD in Inorganic Chemistry in 2006 under the guidance of Prof. Michel Che, in collaboration with Philippe Sautet (ENS-Lyon). She joined the team of H. Toulhoat and P. Raybaud at IFP Energies nouvelles in 2006. She currently holds a researcher position in the Catalysis and Separation Division. Her research interest deals with computational catalysis, in particular surfaces of oxides and supported metals. She co-authored more than 40 publications, one book chapter and one patent.



Pascal Raybaud obtained a PhD in chemistry jointly from Technical University of Vienna (Austria), Paris 6 University (France) and IFP Energies nouvelles in 1998, under the guidance of Profs. J. Hafner, B. Silvi and H. Toulhoat. His research works combined experimental and computational chemistry approaches applied to refining catalysts, hydrogen storage and photocatalytic materials. In 2010, he was awarded the Prize of the Catalysis Division (French Chemical Society). He co-authored more than 90 publications, 12 patents, and is co-editor of the book "Catalysis by Transition Metal Sulfides – From Molecular Theory to Industrial Application" (Editions Technip, France, 2013).

Introduction

Since the 19th century, when "catalysis" was given a definition by J.J. Berzelius, heterogeneous catalysis was at the origin of significant societal advances, materialized by the set-up of major catalytic processes, such as the synthesis of ammonia,^{1, 2} hydrotreatment,³ Fischer-Tropsch synthesis,⁴⁻⁶ catalytic cracking⁷ and reforming,^{8, 9} automotive exhaust treatment¹⁰⁻¹⁴ to name a few. Advanced rationalization studies of catalytic reactivity and surface reactions were undertaken very early, some of them being awarded Nobel prizes, as P. Sabatier¹⁵ (in 1912), I. Langmuir¹⁶ (in 1932) and recently, G. Ertl in 2007.¹⁷ One may however admit that earlier most efficient industrial heterogeneous catalysts such as those used in refining plants were discovered empirically, thanks to a combination of sharp chemical intuition and strong opportunism. For instance, the promoting effect of Co in MoS₂ systems, widely used nowadays in hydrotreating processes, was discovered around WWII only after a large number of trial and error experiments.^{18, 19} Similarly reforming catalysts are the subject of continuous empirical improvements since WWII involving various types of dopants added either on the metallic phase or on the alumina support, the role of which remains however under debate.^{8, 9, 20} Thus, the composition and structure of the industrial catalysts (active phase and support) are generally very complex. Current applied research integrates advanced tools for the discovery of new efficient active phases,²¹⁻²³ which usually brings additional components to the original formulations of heterogeneous catalysts.

Accurate control of the catalytic performance however requires advanced knowledge of the structure of the numerous active sites and of the origin of their catalytic properties, at the atomic scale. This is not an easy task from the experimental point of view, as the respective contributions of each type of site to the spectroscopic or catalytic response are generally convoluted. One may choose two rational approaches to unravel this issue. The first one consists in the elaboration of model catalytic systems, exhibiting a limited variety of sites

of controlled coordination, taking part to a well-defined crystalline network, to isolate their respective structure and implication in catalytic reactions. These model systems can be cleaved single crystals or thin films obtained by surface science techniques,²⁴⁻²⁶ or particles with controlled morphology and narrow size distributions²⁷⁻³⁰ for example. The second approach is based on the development of advanced analytic methods,^{29, 31-34} possibly designed for *in situ* and *operando* experiments,^{35, 36} and of innovative catalytic procedures and reactors.^{22, 37, 38} Of course both approaches can be combined, and have led to significant achievements in the understanding of metallic and oxide surfaces in particular.³⁹

Computational chemistry is a precious and complementary approach to provide a better description and understanding of heterogeneous catalytic active sites at the atomic scale. Thanks to the development of Density Functional Theory (DFT) elaborated by Hohenberg and Kohn (one of the Nobel prize in Chemistry 1998),⁴⁰ it is now possible to apply quantum chemistry for the simulation of simple catalytic systems, as perfectly crystalline zeolites and ideal metal surfaces for example.^{41, 42} Due to high computational requirements, the simulation of more complex catalytic systems as a whole remains however not trivial.

Most commonly used types of models for heterogeneous catalysts were detailed in previous perspectives.^{43, 44} In brief, a piece of the system can be modelled either by clusters of finite number of atoms or by ideal infinite surfaces within periodic boundary conditions. The cluster approach consists in the simulation of a piece of a particle (representing the active phase) from 10 to several tens of atoms. In the spirit of hybrid schemes developed for the simulation of macromolecules by Warshel, Levitt and Karplus (the Nobel Prizes in Chemistry 2014), in particular biomacromolecules,⁴⁵ embedding species can be added in the surrounding to describe, at a lower level of theory, the remaining part of the catalyst particle.^{46, 47} The periodic approach consists in the simulation of an elementary cell, containing from several tens to several hundreds of atoms. The cell is periodically replicated

over three (sometimes two) directions in space for the simulation of a crystal, or of an infinite surface if a vacuum layer is introduced.

By essence, a model of the surface is aimed at, so that quantum calculations are preferentially compared to experiments performed on model systems. When dealing with periodic approaches, ideal cleaved surfaces of catalytic materials or ideal bulk structures of microporous materials are generally considered as models. This is the case for example for simulations of zeolites^{41, 48} or metallic surfaces.⁴³ In the latter systems, low indexes crystallographic orientations depending on the metal crystal symmetry are chosen as relevant for metallic active sites exposed on the particles.^{41, 49, 50} For FCC metals, the most stable (111) terrace led to the most important amount of work. The appropriate choice of specific cleavage orientations (generally with high Miller indexes) also enable the simulation of periodic defects such as steps.^{49, 51} For the study of chemical reactivity at such metallic surfaces, the most convenient way is to start from a bare surface, and to consider low and constant reactant coverage, so as to identify the intrinsic effect of the metal nature and local structure on reaction energies and activation barriers, and possibly deduce some “universal” trends in catalysis.⁵⁰

During the last decade, a great number of theoretical studies have been published in this spirit. This ideal surface approach at low coverage is expected to be powerful and relevant when the chemical state of the catalytically active phase is weakly perturbed by chemical environments: coverage effects, support effects, change of surface chemical composition, etc.. Regarding the degree of complexity reached by the real catalytic systems (either at the industrial scale or the laboratory scale), it is often mandatory to go beyond the ideal surface approach at low coverage. This is particularly true when defects cannot be described by specific cleavage orientations of the bulk materials, such as for low coordinated sites of nano-agregates, extra-framework species or vacancies,⁵²⁻⁶² and when they dominate

the surface reactivity of solids. It is also mandatory to address the complexity of the system for supported catalysts when support effects are suspected to influence directly or indirectly the reactivity.⁶³⁻⁶⁵ This is the case in bifunctional catalysts such as hydroisomerization or hydrocracking where a hydrogenation function is brought by a metallic phase (reduced or sulfided) and a cracking or isomerizing one is brought by the acidic support such as a crystalline zeolite or an amorphous silica alumina (ASA).^{3, 7, 66} In addition, indirect support effect occurs when the size of active nanoparticles becomes sub-nanometric such as in reforming catalysts.⁹ Their electronic and structural properties are expected to be modified by the support. Finally, the ideal surface model at low coverage is not relevant anymore when the reaction conditions modify the chemical state of the catalyst. Several well-known examples illustrate that a metallic surface does not remain purely metallic and tends to become either oxidized under oxygen partial pressure,^{67, 68} or carburized under carbon chemical potential.⁶⁹⁻⁷² Most oxide surfaces become usually hydroxylated when contacted with moisture, which obviously influences their Brønsted/Lewis acidities.^{53, 73-78}

This complexity represents a double challenge for current and future atomic scale's simulation: firstly, one needs to include a sufficiently large number of atoms, arranged in a rational manner – not arbitrarily – to render the variety of surface sites such as Lewis and Brønsted acido-basic sites, defects, etc., which is limited by computational resources and codes performance. Secondly, one has to undertake a highly rational approach to propose a relevant model for a complex system working in given reaction conditions, which modify the chemical state of the surface.

As methodological aspects and challenges of quantum calculations for heterogeneous catalysis were the object of previous perspectives,^{43, 44} we focus here on the the need to take into account the complexity in the molecular models to reach chemical relevance for current or future industrial catalysts. We highlight first principles studies performed in our group,

which recently addressed this high degree of complexity of the catalytic system under reaction conditions:

- amorphization of oxide surfaces on the one hand, with the particular case of amorphous silica alumina (ASA),
- ultra-dispersed mono and multi-metallic catalysts, with the example of subnanometric platinum clusters, possibly doped with tin and/or indium, supported on γ -Al₂O₃.

Both aspects will be discussed in close conjunction with the effect of the surrounding environment: temperature and partial pressures of main reactants, which directly influence the coverage effects.

These two systems are of paramount importance in industrial catalysis. ASA is the acidic support of catalysts involved hydrocracking,^{7, 79} and is also used in the field of biomass conversion,^{80, 81} due to its mild acidic properties. Ultra-dispersed platinum-based catalysts supported on gamma-alumina are involved in dehydrogenation and catalytic reforming processes, inter alia.⁹ The rational and molecular scale approach led to the proposal of original surface sites which revisit some experimental findings but also open avenues for future experiments. The impact of ambient atmosphere and reactive medium is taken into account thanks to a thermodynamic approach. The structural complexity of these systems is also at the origin of an enriched catalytic behaviour for multi-steps reactions. We will show how DFT calculations can also help in this field. Through these two examples, we will propose some challenges and perspectives in the integration of chemical complexity in the simulation of heterogeneous catalysis.

1. General methods

The search for more and more accuracy for reasonable computational cost is a motivation in our field.⁴³ As many groups, we use state-of-the-art methods for the elaboration

of models of heterogeneous catalysts. Most calculations reported in the present perspective were performed in the framework of the Density Functional Theory, using a periodic plane-wave method as implemented in the Vienna Ab initio Simulation Package (VASP).^{82, 83} The exchange-correlation functional was treated within the generalized gradient approximation (GGA) parameterized by Perdew and Wang (PW91)⁸⁴ or by Perdew, Burke and Ernzerhof (PBE).⁸⁵ The projected augmented wave (PAW) method⁸⁶ was used to describe the core-electrons interactions, with energy cutoffs between 400 and 500 eV. Dipolar correction was applied to account for the arbitrary interaction between asymmetric - thus polar - slabs. In some cases, molecular dynamics calculations were undertaken to obtain more stable systems, likely to be more relevant model for the complex systems under study. To account for reactive environment (temperature, partial pressure of H₂O, H₂, hydrocarbon), we undertook thermodynamic calculations, with the assumption that all gaseous species behave like ideal gases. For further details, the reader is invited to read the respective papers.^{20, 87, 88}

Both systems presented in this perspective share a common starting "ingredient", which is the alumina support model developed previously by Digne et al.,^{73, 74} on the basis of the γ -Al₂O₃ bulk model established by Krokidis et al.⁸⁹ The (100) and (110) surface orientation represent about 90 % of the total surface area of the particles. The (100) is the less reactive (in particular the less hydrophilic one), whereas the (110) surface remains hydroxylated up to high temperatures / low water partial pressures.⁷⁷ These surfaces can possibly be chlorinated to promote their acidity. A chlorinated model was also established by Digne et al.⁹⁰ All these surface models were the basis for the simulation of more complex systems, as shown below.

2. Surface models for Amorphous Silica Alumina

Amorphous silica-aluminas (ASA) are composed of variable amounts of silica (SiO_2), alumina (Al_2O_3) and water (H_2O), and are widely used for their acidic character.⁷ Zeolites, which also belong to the aluminosilicate family, are also widely used in catalysis. Being well-defined crystalline materials, the relationship between their structure and acidity was characterized and studied extensively for some decades.⁹¹⁻⁹⁴ By contrast, the lack of long range ordering in ASA hampers systematic characterisation of the local environment around each cationic species. However, these materials are regaining interest for industrial applications, in particular for the enhancement of the selectivity in middle distillates in hydrocracking reactions,^{7, 95} and for biomass conversion.^{80, 81} From a fundamental point of view, the determination and the characterization of the acid sites of ASA remain challenging opened questions. Structural hypothesis are not unanimous between research groups.⁹⁶⁻¹⁰¹ New insights were recently acquired through DFT calculations,^{87, 102-104} leading to a surface model of silicated alumina, which accounts for the presence of original surface sites at the origin of mild acidity. Note that to the best of our knowledge, despite significant effort in the simulation of bulk aluminosilicate glasses in the field of geological glasses,^{105, 106} simulations studies of the surface of ASA was not undertaken before, if we except some earlier attempts to choose “local” models, as aluminosilsesquioxanes.^{107, 108}

2.1. Grafting of silica derivatives on alumina

ASA samples can be synthesised by very different methods,¹⁰⁹ in particular by deposition of organosilanes $\text{Si}(\text{OR})_4$ on $\gamma\text{-Al}_2\text{O}_3$. This method yields silicated alumina with satisfactory control of the amount of silica deposited.¹¹⁰ An exchange reaction is expected to take place with OH groups of alumina¹¹¹⁻¹¹³ followed by hydrolysis. The overall reaction is thus formally equivalent to silicic acid $\text{Si}(\text{OH})_4$ exchange with $\gamma\text{-Al}_2\text{O}_3$ hydroxyls : this general reaction was modelled by Density Functional Theory calculations.

We started with the γ - Al_2O_3 alumina model obtained previously by Digne et al.^{73, 74} (see section 1). The (100) surface of alumina appeared to be the most interesting in terms of amorphisation.⁸⁷ For silicic acid coverage $\theta_{\text{Si}} = 0.5 \text{ nm}^{-2}$, the preferred exchanged configurations lead to the competitive bidentate and monodentate structures illustrated in Figure 1-(a) (top), obtained by exchange mainly with μ_1 -OH, consistently with infra-red experiments.¹¹³

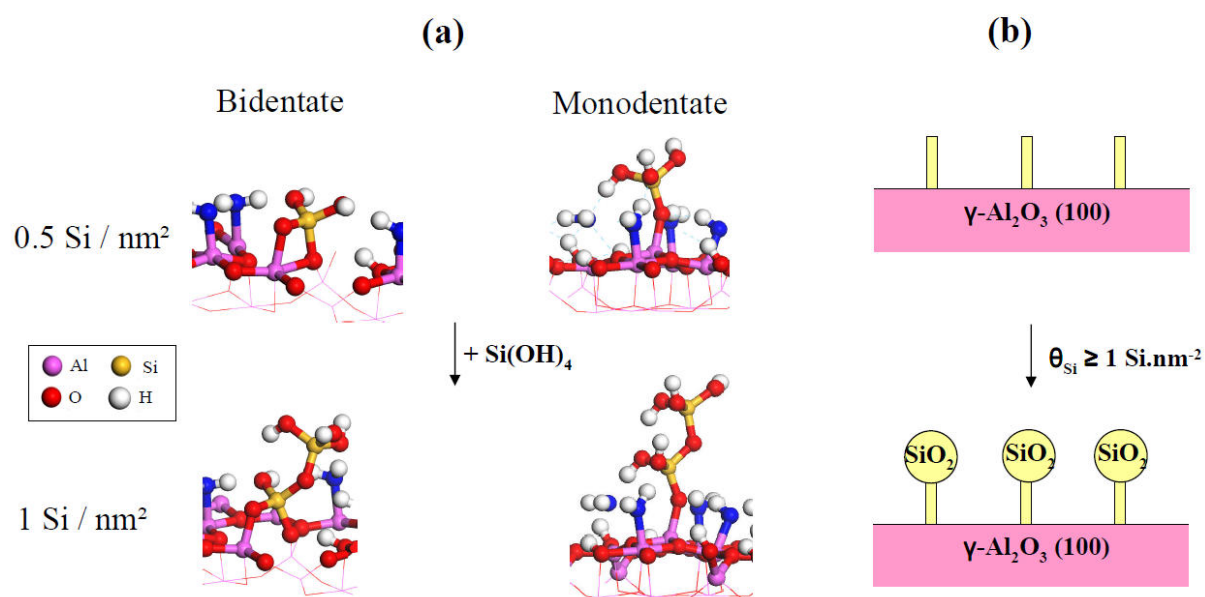


Figure 1. (a) Preferred exchanged structures, calculated by DFT, of Si(OH)_4 on the hydrated $\gamma\text{-Al}_2\text{O}_3$ (100) surface, for monodentate and bidentate configurations, and for $\theta_{\text{Si}}=0.5$ and 1 Si.nm^{-2} . (b) Diagram illustrating the surface state after silicic acid deposition, without any thermal treatment. Adapted from ref.⁸⁷.

Additional silicic acid molecules ($\theta_{\text{Si}} = 1.1 \text{ nm}^{-2}$) condensate with the previously grafted species (Figure 1-(a), bottom), rather than graft onto other alumina OH groups. The condensation reaction energies ($\sim 30\text{-}40 \text{ kJ.mol}^{-1}$) show that increasing the silicic acid content in a wet environment leads to the growth of silica particles in contact with $\gamma\text{-Al}_2\text{O}_3$ (100) by only a few anchoring points (Figure 1-(b)). Thus, in the absence of any thermal treatment, no intimate interaction between silica and $\gamma\text{-Al}_2\text{O}_3$ can be reported on the (100) $\gamma\text{-Al}_2\text{O}_3$ surface.

The effects of thermal treatment were deduced from simulation starting from an epitaxially deposited silica film (with $\theta_{\text{Si}} = 6.4 \text{ Si.nm}^{-2}$) over the $\gamma\text{-Al}_2\text{O}_3$ dehydrated surface,

submitted to a simulated annealing sequence combining DFT and force-field molecular dynamics. The formation of an amorphous phase, and mixing of silica and alumina were observed (Figure 2-(a)).

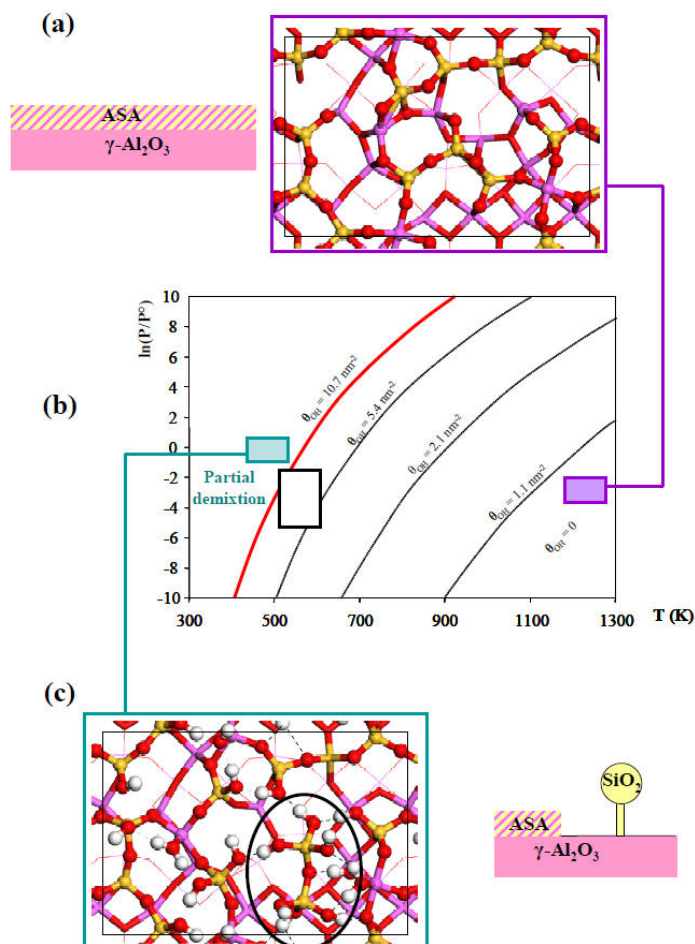


Figure 2. (a) Top view of the fully dehydrated ASA surface model. Side-view scheme of the mixed phase deposited on alumina. (b) Thermodynamic diagram depicting the OH content as a function of the temperature and the partial water pressure. The black rectangular zone corresponds to typical conditions for reactivity applications. (c) Top view of the ASA surface model at $\theta_{\text{OH}} = 10.7 \text{ nm}^{-2}$, the ellipse highlights the silicic acid dimer demixed from ASA upon successive water molecule adsorption, which leads to partial segregation of silica as shown in the scheme. Adapted from ref. ⁸⁷.

Aluminium atoms migrated from the alumina phase to a mixed ASA phase. Released from an octahedral position in pure alumina, they finally exhibit tetrahedral and pentahedral coordination, which is in line with experimental findings from ^{27}Al NMR : the $\text{Al}_{\text{IV}}/\text{Al}_{\text{VI}}$ ratio is higher in ASA than in $\gamma\text{-Al}_2\text{O}_3$,^{98, 114} and Al_{V} exist in ASA.^{114, 115} The crucial impact of thermal treatment for the synthesis of an ASA phase is thus molecularly demonstrated. The

surface obtained exhibits some original Al_{IV} and Al_V likely to behave as Lewis acids, but the generation of Brønsted acid sites requires OH groups.

The surface state of ASA was thus determined as a function of the temperature and partial water pressure (Figure 2-(b)), by simulating successive adsorption of water molecules. Silanols are preferentially generated over Al-OH groups. For high water contents (Figure 2-(c)), silicic oligomers demix from the ASA phase. These types of oligomer are expected to segregate so that part of the mixed ASA phase is lost. In particular, calculations predict a systematic trend to demixing at room temperature (unless some kinetic limitations occur), illustrating again the most important role of thermal treatment in the stabilisation of a mixed aluminosilicic phase.

2.2. Hydroxyl groups present on the ASA surface models

For typical analytical and reactivity conditions, surface models exhibiting 5.4 and 6.4 $OH.nm^{-2}$ (black rectangle in Figure 2-(b)) are representative of the real surface state. On these surface models (Figure 3-(a) and (b)), various species are identified: Al_{IV} and Al_V atoms, as well as several kinds of hydroxyls. In particular, one bridging Si-(OH)-Al site (Figure 3-(c)) is present. Silanol bonded to aluminium atoms (Al_{VI} and / or Al_V) via structural Si-O-Al bridges are found (Figure 3-(d)). We called these groups Silanol-Al.

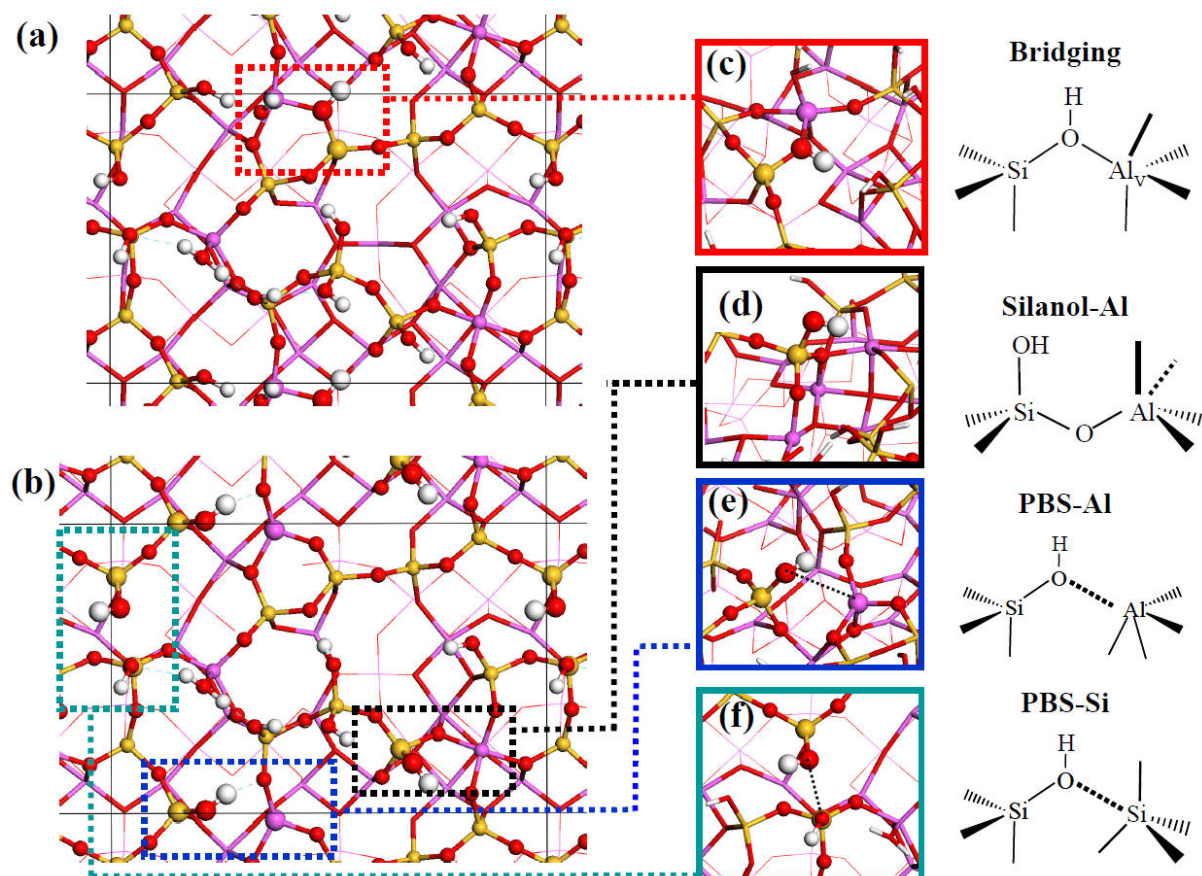


Figure 3. Top view of the ASA surface model for (a) $\theta_{\text{OH}} = 6.4 \text{ OH.nm}^{-2}$, (b) $\theta_{\text{OH}} = 5.4 \text{ OH.nm}^{-2}$. (c) Bridging OH group. (d) Example of Silanol-Al group. (e) Example of PBS-Al (PBS: Pseudo-Bridging Silanol). (f) Example of PBS-Si.

Several silanols in interaction through space (no Al-O covalent bond) with one acceptor Al_{IV} or Al_{V} atoms are also present (Figure 3-(e)). These we called Pseudo-Bridging Silanols (PBS),^{87, 102, 103} in particular PBS-Al, when Al acts as the "acceptor" atom. In some cases, a silicon atom may also play the role of the acceptor (Figure 3-(f)), as seen with the so-called PBS-Si group. Note that since then, PBS-Al-like sites were suspected on silicated alumina from experiments.¹¹⁶

This variety of OH group environments suggested by the model explains the complexity of the infra-red spectra of ASA. The vibration frequencies of OH groups on the ASA surface model were indeed calculated and compared to experiments (Figure 4).¹⁰³ The Si-OH frequency, calculated and observed near 3740 cm^{-1} in silica,¹¹⁷ is lowered when the silanol is in close proximity (Silanol-Al and PBS-Al) with an Al atom. The difficult

observation of zeolite-like bridging OH groups on ASA is also explained by the lower thermal stability than in zeolites, as well as the dominant contribution of hydrogen-bond donor OH groups in the same spectral region. This study has a double interest: together with the assignment of the FTIR spectra of ASA samples, a validation of the theoretical model is obtained.

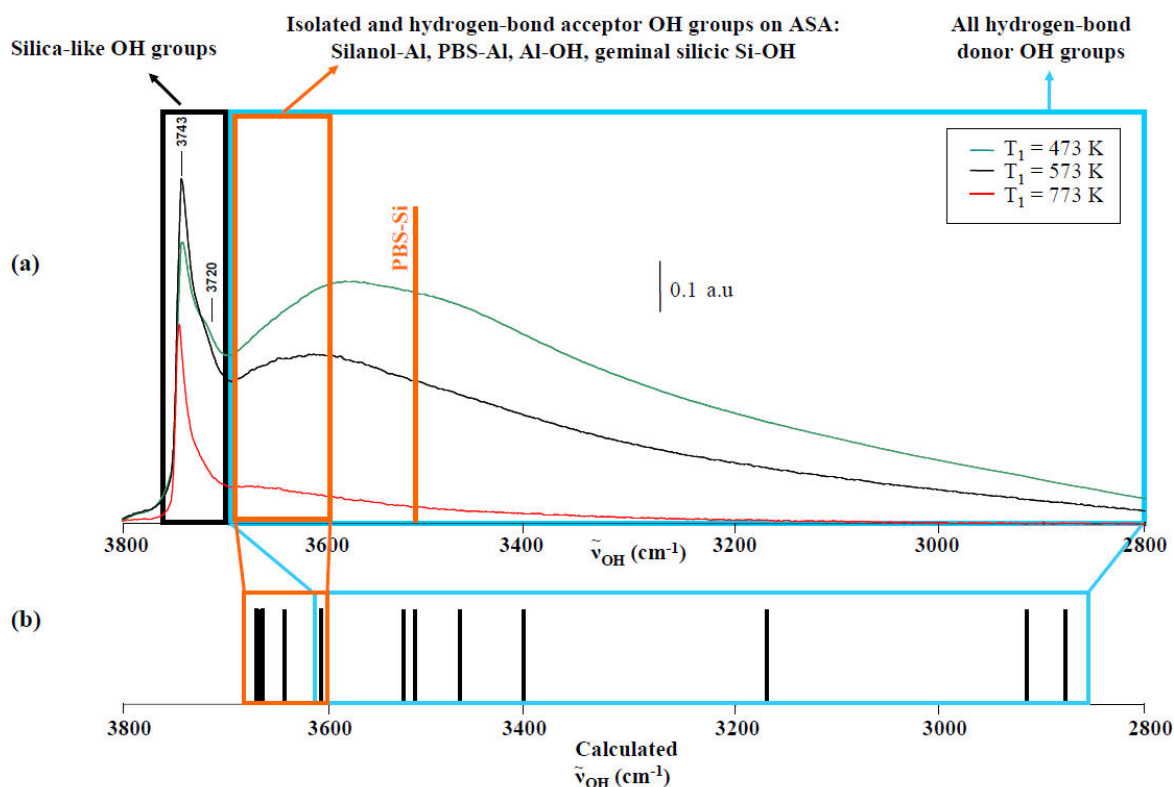


Figure 4. (a) Experimental infrared spectrum of ASA, in the O–H stretching zone, for the ASA sample evacuated at 473, 573, or 773 K. The assignment proposed is based on the computational results. (b) Calculated O–H vibration frequencies for the various sites present on the ASA model. Adapted from ref. ¹⁰³.

2.3. Acidity of OH groups on ASA : on the dominant role of the stability of the conjugated base

Thanks to this model, the independent behaviour of each site can be inferred with regard to basic probe molecules. Zeolite-like bridging Si-(OH)-Al groups, similar to those of protonic zeolites, are often referred to as the most acid sites of ASA^{99, 118-120} but their existence is questioned by other authors^{96, 97} due to the absence in the ASA IR spectra of the

typical well-defined O-H bands observed in zeolites. Our DFT calculations show that they can exist on the ASA surface,⁸⁷ even if the coordination number of their aluminium atom is not systematically equal to four. Silanols bonded to low coordinated aluminium atoms by a Si-O-Al bridge were presented as the most acidic Brønsted sites by Crépeau and co-workers,⁹⁸ depending on the number and coordination of Al. These sites are related to Silanol-Al proposed within the DFT model.

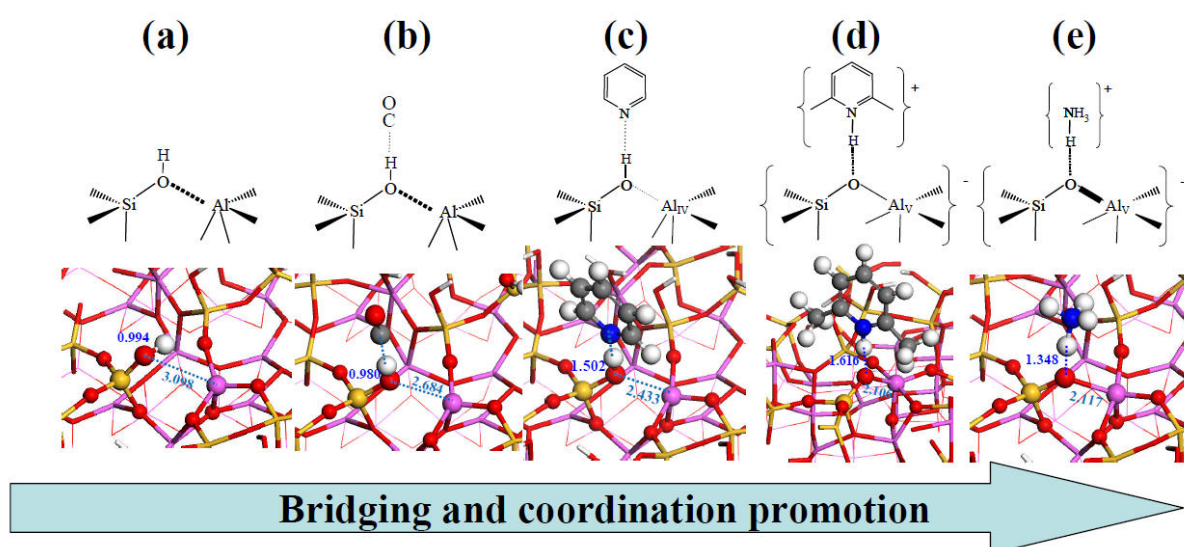


Figure 5. Behaviour of aluminic Pseudo-Bridging Silanols (PBS-Al) towards basic probe molecules: (a) No probe molecule, (b) CO, (c) pyridine, (d) lutidine, (e) ammonia. O \cdots H distances and O-H bond lengths (\AA) are given in blue, O \cdots M distances and O-M bond lengths (\AA) in black. Adapted from ref. 102.

The adsorption of probe molecules of various basicity was then simulated¹⁰² on the four sites depicted in Figure 3: CO, pyridine, lutidine and ammonia. All nitrogenated probe molecules are converted in their protonic conjugated acid on the bridging Si-(OH)-Al group, with adsorption energies lower than protonic zeolites. Conversely, Silanol-Al was unable to protonate any of the molecules under study. PBS-Al exhibits more interesting chemical behaviour, as illustrated in Figure 5: probe molecule adsorption induces a tilt of the oxygen of PBS-Al in the direction of the aluminium atom. This phenomenon is reinforced by

increasing the probe molecule basicity, with protonation of lutidine and ammonia. This is accompanied by the formation of a new Al-O bond, increasing the coordination of the acceptor Al atom from four to five. This phenomenon relates to the proposal put forward by Trombetta et al.⁹⁶ based on experiments of nitrogenated molecules on ASA monitored by FTIR. More surprisingly, the same kind of behaviour was found for PBS-Si, with formation of a Si_v. Consequently, together with bridging Si-(OH)-Al groups, PBS-Si appears to be one of the most acidic Brønsted sites on the ASA surface, with higher protonating ability than PBS-Al (pyridinium ion being generated on PBS-Si).

A more detailed analysis was performed in the case of lutidine adsorption, on all sites of the ASA surface model.¹⁰³ As PBS and bridging OH-groups, water molecules adsorbed on aluminum atoms exhibit interesting proton transfer ability. This is consistent with previous experimental proposals.^{100, 121} In a general manner, we showed that the main factor governing the proton transfer ability of acid sites of ASA is the stabilisation of the conjugated base (of the acid site), either on formation of Al-O or Si-O bonds, or by cascade proton transfer,¹⁰³ as explained in figure 6. In addition, the properties of the modelled ASA's OH groups were compared to that of an ideal bridging OH group within mordenite. The lower Brønsted acidity of ASA compared to zeolites was assigned to the lack of electrostatic confinement effect. This result may have a significant impact on the role of pore size on the reactivity and selectivity in hydrocracking reactions, which will be the object of future investigations.

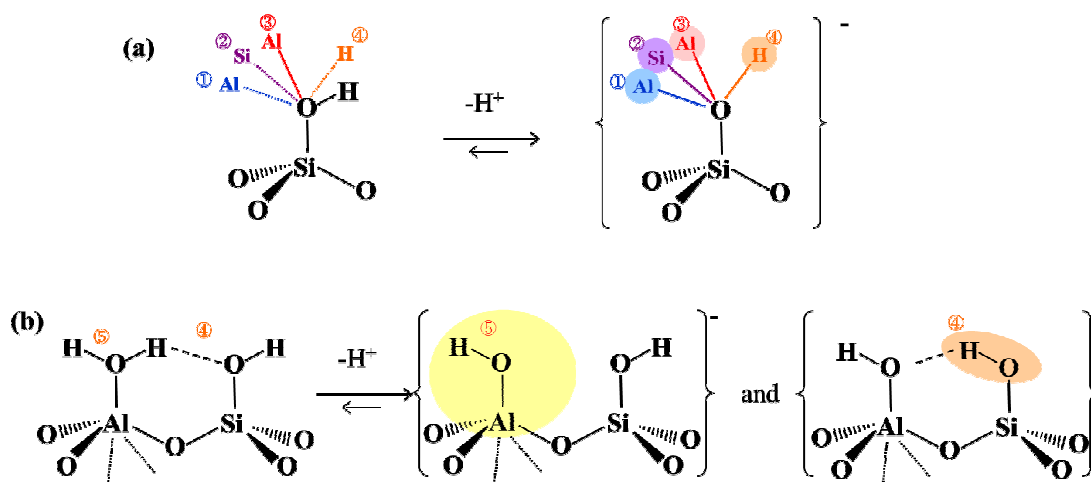


Figure 6. Synopsis of the various Brønsted acid sites on the ASA surface: (a) PBS-Al (①) and PBS-Si (②) are deprotonated with the formation of new Al-O and Si-O bonds. Bridging OH-groups (③) are deprotonated thanks to the existence of the Al-O bond. Silanol in the vicinity of labile protons (④, see also (b)) is deprotonated with cascade proton transfer from the water molecule. (b) Acidity induced by water molecules adsorbed on Al atoms: proton transfer by the water molecule itself (⑤) or cascade proton transfer to the neighboring silanol (④, see also (a)). Adapted from ref. ¹⁰³.

We also investigated in more details the interaction of CO as a probe molecule on all sites of the ASA model,¹⁰⁴ as this molecule is being used since many years to characterize experimentally the acidity of various materials,¹²²⁻¹²⁵ including ASAs.^{56, 96-99, 120, 126} Common sense suggests that the more positively charged the proton, the more acid a surface OH-group. CO is able to probe charges along the surface because of its dipolar nature. This perturbation induces a shift of the CO infrared stretching vibration usually measured by FTIR. The CO stretching vibrational frequency is indeed shifted ($\Delta\tilde{\nu}_{\text{CO}}$) and depends on the adsorption sites, which are both Brønsted and Lewis acid sites. It is generally admitted that the more acidic the adsorption site, the larger the shift of CO vibration. Nonetheless, we found that CO probes the surface electrostatic field, producing a vibrational Stark effect, which does not depend solely on the Brønsted acid character of the protons (this latter parameter being quantified by the proton transfer ability to lutidine, figure 7). On the ASA surface, the higher calculated shifts were assigned to some PBS-Al groups, likely due to the high electrostatic

field imposed by aluminum cations. This shift ($\sim 35 \text{ cm}^{-1}$) is in good agreement with the signal experimentally assigned to "strong Brønsted acid sites".^{56, 98, 120}

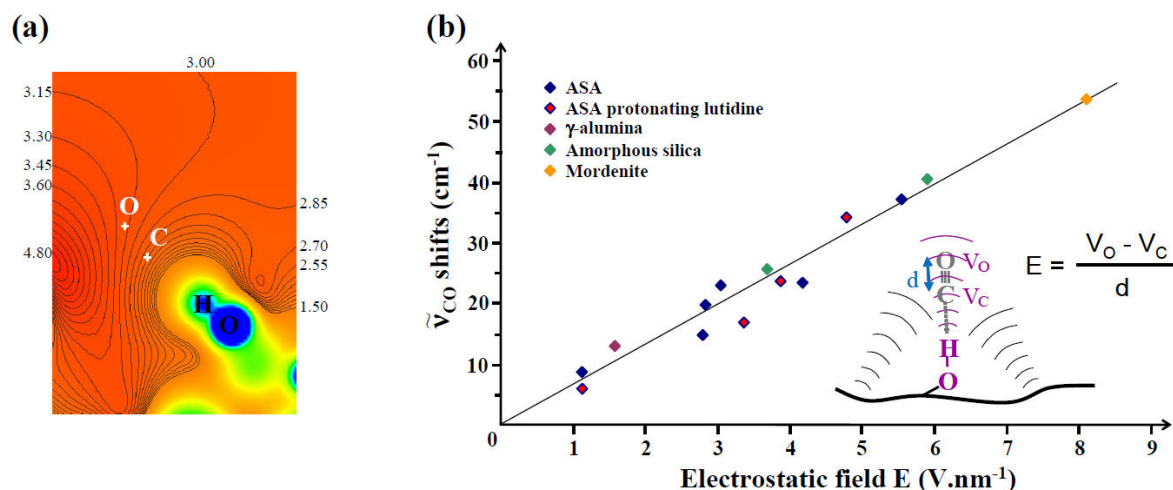


Figure 7. (a) Electrostatic potential isosurfaces projected in the plane defined by the CO and OH atomic positions (values in V), for CO adsorbed on one PBS-Al site; (b) CO frequency shift (cm^{-1}) against electrostatic field potential (V.nm^{-1}): $\Delta\tilde{\nu}_{\text{CO}} = 6.4 E$ ($R = 0.91$). Adapted from ref. ¹⁰⁴.

3. Models of ultra-dispersed catalysts : noble metals supported on $\gamma\text{-Al}_2\text{O}_3$

Platinum supported on γ -alumina ($\gamma\text{-Al}_2\text{O}_3$) is a prominent catalyst involved in many different fields such as the treatment of automobile exhaust,¹⁰ catalytic reforming,⁹ alkane dehydrogenation,¹²⁷ and biomass conversion.⁸⁰ In many catalytic processes, due to economic constraints, the optimal use of each Pt atom as an active site is critical and thus, it is sought to reach subnanometer particles' sizes while keeping their metallic properties. The γ polymorph of alumina, possibly chlorinated, is the most widely used in industry due to its advantageous porosity, surface area and chemical properties.¹²⁸ Catalytic reforming is one of the applications of interest where subnanometer size particles are of great importance and where the effect of the support is also predominant.⁹ In this case, Pt is usually highly dispersed (content lower than 1 wt %). The level of complexity of these catalysts is high, due to the subnanometer size of the particles, to the presence of dopants in the metallic phase (other

metals such as Sn) and on the support (chlorine or indium for example). The reaction network in which they are involved is also very complex, due to the bifunctional nature of the system (metallic and acidic phase) and the various desired (isomerisation, dehydrogenation, dehydrocyclisation) and undesired (coking, hydrogenolysis, cracking) reactions.

HRTEM¹²⁹⁻¹³³ and STM^{134, 135} provide precious insights for 2D supported metallic structures, while X-Ray absorption spectroscopy (XAS)^{33, 133, 136-140} was successfully applied to get 3D structural information. However these techniques do not provide a single unambiguous particle model, so that many questions remain open about these highly fluxional structures, under reactant pressure. To get a deeper insight in the structure and behaviour of active sites in catalytic reforming, we performed DFT calculations coupled to a thermodynamic model. The complexity of the industrial multi-metallic catalyst was taken into account by a step-by-step approach, dealing first with monometallic, then multimetallic systems.

Several first-principles studies of Pt/alumina systems based on *ab initio* calculations were reported in the literature by other research groups. They differ first in the nature of the alumina surface model. Very often, ideal α -Al₂O₃ surfaces were considered.¹⁴¹⁻¹⁴⁸ The abundance of Al_{IV} atoms in γ -Al₂O₃, which are absent in α -Al₂O₃, however makes the explicit study of the γ polymorph needed. The hydroxylation state of the support was addressed in some studies,¹⁴⁷⁻¹⁴⁹ however, its influence on the morphology of a polyatomic cluster was not investigated. In general, the simulated sizes remained well below the real sizes of high dispersion oxide-supported metal clusters with diameters distributed around 1 nm. Only recently, supported Pt₁₀¹⁵⁰ and Pt₁₉¹⁵¹ particles were simulated, but with limited investigation of the morphology of the clusters. Our work, presented below, is thus one of the first achievements of morphology definition of platinum clusters of reasonable size (Pt₁₃)

supported on a realistic γ -Al₂O₃ surface model. We also addressed for the first time supported PtSn systems,¹⁵² which was followed by complementary research of other groups.¹⁵³

3.1. Size and morphology effects in ultra-dispersed platinum catalysts

Relevant models of monometallic platinum particles supported on dehydrated, hydroxylated and chlorinated γ -alumina were firstly elaborated,^{154, 155} based on alumina support models presented in section 1, and on models of metallic non-supported clusters.¹⁵⁶ Platinum clusters containing 13 atoms were considered as being representative of highly dispersed platinum catalysts with particle size close to 1 nm. Symmetric morphologies, as cuboctahedron or icosahedron, appeared to be less favourable than less symmetric structures in gas phase (Figure 8-(a)), as biplanar structures, or irregular edifices obtained by simulated annealing sequences.¹⁵⁶ Smaller particles (from 1 to 5 atoms) were also considered, as HRTEM suggest the occurrence of atomically dispersed Pt species.^{131, 132} The alumina (100) surface is generally dehydroxylated in catalytic reforming conditions, whereas the (110) is still hydroxylated,^{74, 77} possibly chlorinated.⁹⁰ For isolated clusters, the following general rule holds: the bigger the size, the more stable the cluster (figure 8-(b)).

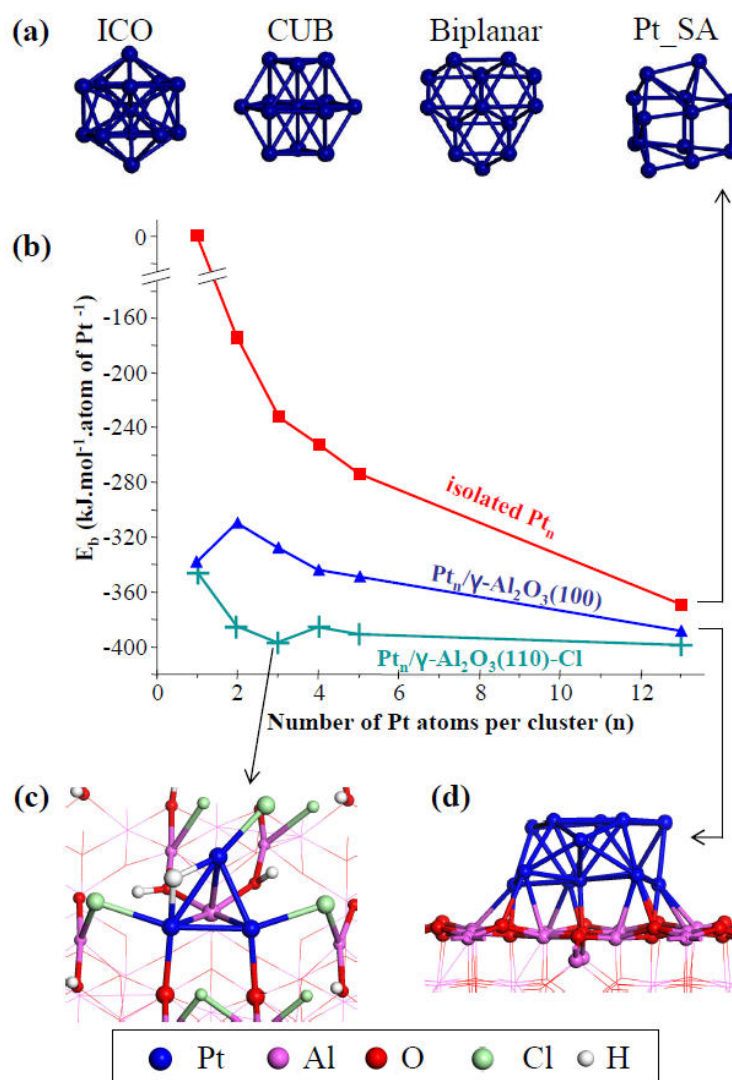


Figure 8. (a) Some isolated Pt_{13} clusters studied in ref. ¹⁵⁶: icosahedron, cuboctahedron, biplanar cluster and structure obtained by a simulated annealing sequence. (b) Calculated binding energy (including Pt-Pt cohesion and metal-support interaction) of Pt_n clusters, isolated or supported on $\gamma\text{-Al}_2\text{O}_3$. Adapted from ref. ¹⁵⁵. (c) Most stable Pt_3 cluster supported on chlorinated $\gamma\text{-Al}_2\text{O}_3$ (110) surface. Adapted from ref. ¹⁵⁵. (d) Most stable Pt_{13} cluster supported on dehydrated (and dechlorinated) $\gamma\text{-Al}_2\text{O}_3$ (100) surface. Adapted from ref. ¹⁵⁴.

By contrast, DFT calculations performed on supported Pt_{1-13} clusters showed the significant impact of the rearrangement and migration of surface species (protons, hydroxyls, chlorine) for the stabilization of the smallest Pt clusters.¹⁵⁵ This is mainly explained by the anchoring of the clusters to the surface via Pt-O and Pt-Al bonds. Taking into account the migration of such surface species, Pt clusters are more stable on the hydrated and chlorinated (110) surfaces than on the dehydrated (100) surface. On the chlorinated (110) surfaces, Pt_3 corresponds to a

local energy minimum (Figure 8-(b) and (c)), even lower than Pt₁₃. This stability of Pt₃ would explain an increase of the activation barrier to form larger clusters, thus limiting sintering, thanks to chlorine.^{137, 157}

3.2. Hydrogen coverage effects on the structure of Pt₁₃/γ-Al₂O₃

In a second step, the reactivity of hydrogen towards platinum was investigated on the Pt₁₃/γ-Al₂O₃(100) system.⁸⁸ Hydrogen is indeed present in the reactive medium, in particular in catalytic reforming,⁹ and titration methods aiming at quantifying the dispersion of the platinum particles often involve hydrogen adsorption.¹⁵⁸

On the γ-Al₂O₃(100) surface, in the absence of hydrogen, the Pt₁₃ cluster preferentially lies in the "biplanar" (BP) morphology (Figure 8-(d)) and maximizes the metal-support interaction through Pt-O and Pt-Al bonds.¹⁵⁴ The calculations show that this structure presents a strong affinity towards hydrogen. Most stable structures for given hydrogen coverage (from 1 to 36 hydrogen atoms per cluster) were identified thanks to *ab initio* molecular dynamics. A thermodynamic diagram was constructed, providing the surface state as a function of the temperature and hydrogen partial pressure (Figure 9-a). The increase of hydrogen coverage may reach a H/Pt atomic ratio greater than 1.4, which induces a cluster reconstruction from the BP to a cuboctahedral (CUB) morphology.

H uptake of the supported Pt₁₃ cluster is higher than that of extended Pt(111) and Pt(100) surfaces. For example, at P(H₂)=P^o=0.1 MPa, ideal surfaces exposed by large particles are depleted from H atoms at T > 900 K, whereas the Pt₁₃ cluster still contains 6 H atoms. This illustrates the non-relevance of ideal surface models for depicting the adsorption thermodynamics on subnanometric clusters, and also the importance of considering H coverage effects for the description of ideal surfaces in operating conditions, as θ_H deviates from 0 ML for a large set of (T, P(H₂)) conditions.

3.3. Hydrogen coverage effect on the stability of intermediates of ethane dehydrogenation on Pt₁₃/ (100) γ -Al₂O₃

Then, to understand the impact of hydrogen in the catalytic reactions, in particular alkane dehydrogenation, we performed a DFT study of the stability of C_xH_y (x = 1 or 2 and 0 ≤ y ≤ 5) intermediates, likely formed upon activation of ethane considered as a model molecule for probing C-C and C-H bond scission.²⁰ Symmetric (one H removed on each C atom) and dissymmetric (H removed first on the same C atom) dehydrogenation elementary steps were compared, as well as C-C bond breaking with CH₄ release. Calculated Gibbs free energy profiles at 800 K (representative of reforming conditions) for the transformation of ethane allowed the quantification of the relative stability of C_xH_y species relevant for dehydrogenation and hydrogenolysis pathways as a function of reaction conditions. The impact of the J = P(H₂)/P(ethane) ratio (J = 0.01, 1, 10 and 100) was studied (Figure 10). According to the DFT and thermodynamic calculations, intermediate J values between 1 and 10 correspond to the optimal balance between the two dehydrogenation pathways, the C-C bond scission and formation of CH₄. Simultaneously, ethynylidyne (CCH₃ in Figure 10), considered as a dead end intermediate, is thermodynamically less stable with respect to ethylene as soon as J becomes greater than 1. Within a similar range of J, hydrogenolysis

reaction is also promoted due to the simultaneous stabilization of monocarbonaceous species on the platinum clusters with high hydrogen coverage. Regarding acetylene, its stability is more affected by the increase of J (thus of $P(\text{H}_2)$) than less dehydrogenated compounds. Moreover, the most stable cluster morphology when acetylene is adsorbed at $J=1$ for example, is no longer the biplanar one but the CUB one (Figure 10).

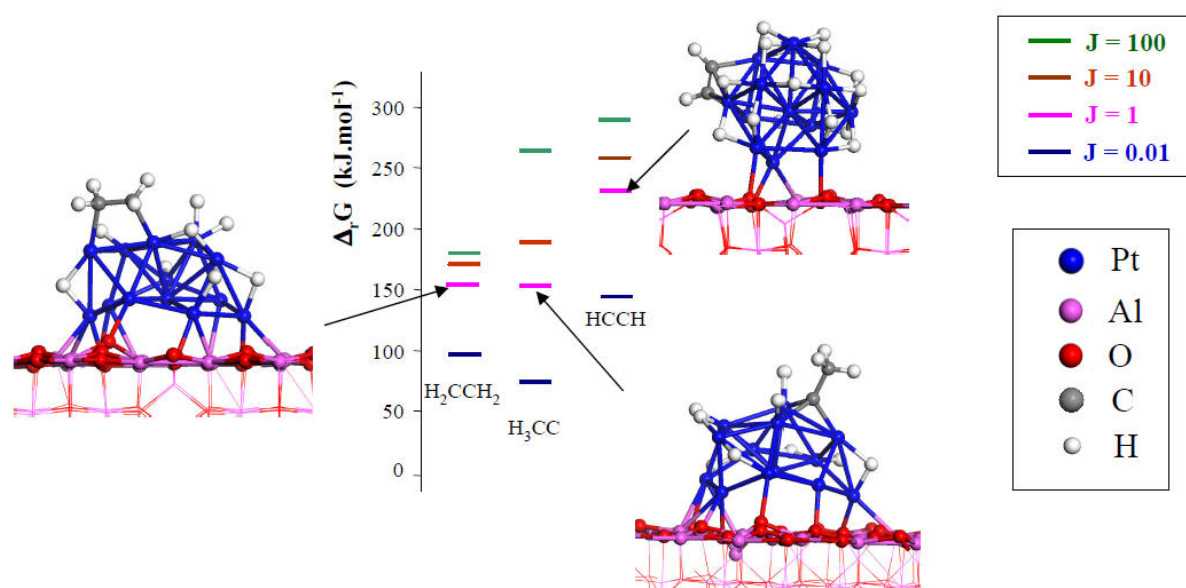


Figure 10. Relative stabilities (Gibbs free energy of reaction of ethane) of adsorbed ethylene (H_2CCH_2), ethylidyne (CCH_3) and acetylene (HCCH) on Pt_{13} supported cluster at various $J = P(\text{H}_2)/P(\text{C}_2\text{H}_6)$ values. Insets : illustrations of structures at $J=1$. Adapted from ref. ²⁰.

As a consequence, we were able to identify and quantify the interval of process conditions to be used for moderate dehydrogenation of ethane into ethylene avoiding further dehydrogenation, ethylidyne formation, hydrogenolysis and coke formation as targeted in process conditions.^{8, 166, 167}

From a more general point of view, such hydrogen coverage effects also impact significantly the behaviour of ideal surface, although it is often overlooked on these simple systems. For instance, in selective hydrogenation of butadiene into butene, it has been shown

that the competitive adsorption of hydrogen also significantly modifies the adsorption mode and thermochemistry of reactants and products on ideal Pd (111) and (100) surfaces.¹⁶⁸

3.4. Towards multi-metallic systems : $\text{Pt}_x\text{Sn}_y/\gamma\text{-Al}_2\text{O}_3(\text{In})$

The next step for a more accurate modelling of the real reforming catalyst is to consider the multimetallic nature of the catalysts: bi-metallicity of the active phase and dopants in the alumina support. We recently undertook this theoretically by focusing on PtSn formulations, possibly with Indium as co-doping element present in the support as In^{3+} (Figure 11).¹⁵² While tin is shown to decrease the metal-support interaction as compared to pure platinum, indium compensates part of the interaction loss, which results in a stabilization of the bimetallic PtSn nano-cluster.

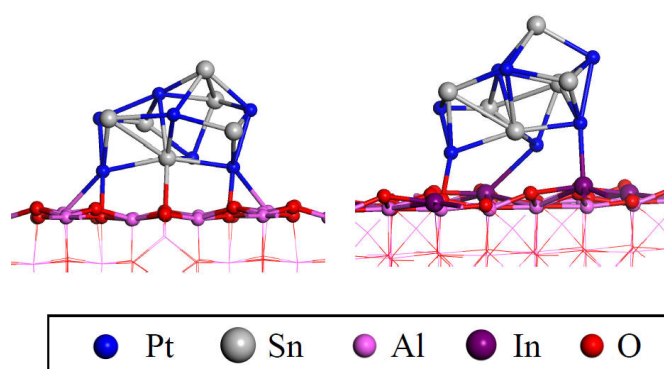


Figure 11. Models of supported PtSn catalysts, without (left) or with (right) indium incorporated in the support. Adapted from ref. ¹⁵².

4. Challenges for the realistic simulation of complex catalytic systems in catalytic conditions

4.1 Current challenges in the simulation of complex aluminosilicate catalysts

The next step toward the understanding of the milder acidity of ASAs as compared to zeolites is the simulation of chemical reactivity, for the conversion of various molecules,

involving the simulated Brønsted acid sites of ASA. As can be inferred from the adsorption of lutidine (see previous section), and from previous kinetic modelling of phenantrene hydrocracking,^{169, 170} confinement effect (stronger within zeolites) will play a key role in proton transfer reactions. We are currently investigating the cracking of alkenes as model reactions for the genesis of carbenium species, and as topical for industrial applications (cracking, hydrocracking). The calculation of reaction rates, including enthalpy and entropy contributions, will be crucial both for the validation of the models (by comparison with experiments) and for the establishment of acidity scales within the family of aluminosilicates. More generally, the transferability of acid site structures, electrostatics and reactivity, to other complex aluminosilicate structures, needs to be understood, in particular thanks to *first principles* calculations including van der Waals corrections (within the Grimme formalism for instance). To name a few, aluminated silica or ASAs obtained by cogelification of aluminium and silicon precursors,¹⁰⁹ amorphous microporous aluminosilicates obtained by aerosol techniques,¹⁷¹ internal surface of organized mesoporous silicas doped with Al,¹⁰⁹ defects of dealuminated – desilicated zeolites¹⁷² and external surfaces of zeolites (at the origin of the so-called “pore mouth” catalysis^{173, 174}) are poorly defined systems at the atomic scale, which need detailed investigations. Likely, Pseudo-Bridging Silanols could be found as relevant acid sites on all those amorphous systems, with variable Si-O-Al angle value and/or variable Al coordination number. Such nature of active site is the first parameter governing acidity. In addition, the confinement effect (van der Waals and electrostatic) induced by tunable mesopore’s sizes is the second parameter driving the acidity strength at the mesoscale. These combined effects still need further rational and quantified theoretical investigations in order to help for the better control of targeted activity and selectivity in industrial reactions such as isomerization and (hydro)cracking.

4.2 Current challenges in the simulation of ultra-dispersed catalysts

DFT calculations appear as an appropriate tool to rationalize the behaviour of complex metallic systems at the molecular scale. Experiments are challenged by proposals coming from our studies.^{140, 165} Experimental characterization is currently being performed to validate some key-features of our theoretical study, in our team and other research groups.¹⁴⁰ The impact of tin on the interaction with hydrogen is also being investigated. Other perspectives are oriented towards the reactivity of such particles with alkanes exhibiting longer chain length.

More generally, the challenges in the field are the appropriate simulation of the multi-component nature of the system, taking into account non-reduced metal toms, dopants and additives, and their impact on the chemical reactivity of the particles within complex reaction networks, involving various types of reactants (hydrocarbons, oxygenates, pollutants, etc.). Throughout such studies, the impact of the reconstruction of the particles should be taken into account.

It remains rather difficult to conclude if theoretical studies based on infinite metallic surface models and deriving so-called “universal” trends (as mentioned in Introduction) can be applied to such multi-component catalysts. To the best of our current understanding, we suggest to remain cautious when using simplified structure-activity relationships in the case of highly dispersed catalysts because the risk of missing the chemical cornerstone of the catalysts is always present.

4.3 General challenges

The previous examples highlight that modelling complex catalytic systems at the atomic scale remains a current challenge, notwithstanding the significant improvement of the efficiency of computational tools in the past decades. Indeed, this research area would not be

possible the exponential increase of computing architectures performances and the significant developments of efficient quantum physics software algorithms.¹⁷⁵ At the same time, a continuous improvement of the accuracy in the determination of the energy and geometry of a given system is achieved by quantum calculation.⁴³ However, undertaking a rational approach to propose a relevant – and not just arbitrary - model, remains a limiting step in this field.

Ideal surface approaches or derived descriptor approaches have the advantage of being simpler and quicker methods, opening the door of the prediction based on periodic trends.^{50, 176-180} They rationalize first screening approach that could be sustained by high throughput experimentations, during the search of a new catalytic formulations for a specific reaction.¹⁸¹ However, this can only be the first order level of computational assistance to the development and improvement of catalysts, which then need a finer molecular scale description of the real catalytic systems beyond the first order level. Thus the right level of complexity must be considered to allow further progresses in the field.

The main perspective of the works presented here is to gain an ever more relevant level of complexity in the simulated systems, so as to provide an optimal model and accurate chemical descriptors valid for industrial catalysts. For example, doping elements or cations and anions issued from the precursors during synthesis on alumina based supports, are known to influence the catalytic properties. Regarding ultra-dispersed platinum-based catalysts, the detailed role of promoters and the impact of their oxidation state (in particular for Sn) should be taken into account. It may also be of crucial interest for industrial catalyst to get a better quantitative understanding on the stability and reactivity of such multi-metallic nanoparticles on modified alumina surfaces (for example silica-alumina). This would help to provide a control at the molecular level of the balance between Brønsted acid sites and metallic sites, which is of fundamental and applied interest for bifunctional catalysts.⁷⁹

One future guideline for such a research is the simulation of all steps of the synthesis and activation procedure of the studied catalysts. In particular, challenging perspectives are the simulation of the solid-liquid interface between the support and the synthesis solutions with significant dynamic solvent effects, possibly charge separation,¹⁸²⁻¹⁸⁴ as well as calcination / reduction steps where the mobility of active phases is high. In particular, the use of state-of-the-art (ab initio or force field based) molecular dynamic strategies will be key in this field. However, it must be stressed that developing the optimal techniques and approaches to better understand chemical phenomena taking place at solid-liquid interfaces remains a challenge not only for theoreticians but also for experimentalists.¹⁸⁵

In this spirit, once accurate models are established for a given catalyst, considering realistic reaction media and the interaction of the catalysts with each component of the gaseous or liquid phase is a complex task.^{186, 187} We illustrated how temperature and pressure effects can be taken into considerations in the simulation, but complex mixture of large molecules are sometimes involved in real reactions. A quantum tool is probably not the most appropriate one to describe the reactivity of such systems: reactive force-field can be one – although not trivial – solution.¹⁸⁸

Finally, understanding and predicting the macroscopic catalytic performance also require to take into account the limitations induced by the combined effects of kinetics, diffusion, convection, local evolution of the temperature and pressures / concentrations. Such a global process can only be modelled thanks to a multiscale approach, integrating quantum descriptors, kinetic modelling and reactor models.^{43, 189-191} For this purpose, collecting systematic DFT data as a function of surface coverage imposed by reaction conditions is necessary. Significant achievements were reported in this field, but usually starting from DFT models of ideal metal¹⁹²⁻¹⁹⁴ or oxide^{189, 195} surfaces. Integrating data for more and more

realistic and coverage dependant DFT models will provide improved description and prediction abilities for catalytic developments.

5. Conclusions

The objective of the present paper was to illustrate the need for accurate models of heterogeneous catalysts, obtained by *ab initio* calculations, which take into account, as far as possible, the complexity of the real catalytic system. To exemplify such an approach, we focused on two systems which has attracted more attention recently in our research work, by the mean of Density Functional Theory calculations : amorphous silica alumina surfaces and sub-nanometer platinum particles, possibly doped, supported on gamma-alumina. These two systems are challenging as they are of significant fundamental and industrial interests, and also due to their complexity, inherent to multi-element composition, structural disorder, and small particle size. Climbing the ladder of complexity, a step-by-step investigation led us to propose rational models of such systems. Extended comparison with the most advanced experimental characterizations is the key for the validation of these models. Atomic insights are then provided, which are not easily reached by experimental techniques only, even cutting-edge ones such as *in situ* XAS or operando IR. In particular, pseudo-bridging silanols were proposed as key active sites on amorphous silica-alumina, whereas a hydrogen-induced reconstruction of platinum particles is anticipated thanks to DFT calculations. This latter example addresses probably one of the highest levels of complexity for a catalytic system: it combines a system with no symmetry, a nano-particle deposited on a support, which is highly sensitive to reaction conditions and support effects. For such systems, quantum descriptors used in the so-called “universal” trends evaluated at ultra low reactant coverage on ideal (infinite) surfaces must be considered with great care. Dedicated theoretical investigations compared with well-defined experiments are certainly mandatory to identify on what can be

defined as relevant, if not “universal”, quantum descriptors. However, even if future experimental investigations may reveal some interesting catalytic systems which do not match with the so-called “universal” trends proposed nowadays, we hope that the present perspective have highlight alternative routes for simulation approaches to tackle these “non universal” cases by considering their own complexities.

6. Acknowledgments

We warmly thank Hervé Toulhoat (IFP Energies nouvelles) and Philippe Sautet (Ecole Normale Supérieure de Lyon) for long-lasting collaborations on some of these topics. Fruitful discussions with partners from theory and experiments are acknowledged, in particular with D. Costa (Chimie Paris Tech), M. Digne, A. Chaumonnot, M. Caillot V. Moizan-Baslé, P. Avenier, S. Lacombe, A. Jahel (IFP Energies nouvelles), J. van Bokhoven (ETH Zürich). We are indebted to former post-doc and PhD collaborators at IFP Energies nouvelles, namely F. Leydier, C.H. Hu, C. Mager-Maury and G. Bonnard for collaborative work reported in the present perspective.

7. References

1. R. Schlögl, *Angew. Chem. Int. Ed.*, 2003, **42**, 2004-2008.
2. J. W. Erisman, M. A. Sutton, J. Galloway, Z. Klimont and W. Winiwarter, *Nature Geosci*, 2008, **1**, 636-639.
3. P. Raybaud and H. Toulhoat, *Catalysis by Transition Metal Sulphides, From Molecular Theory to Industrial Application*, Technip, Paris, 2013.
4. J. L. Casci, C. M. Lok and M. D. Shannon, *Catal. Today*, 2009, **145**, 38-44.
5. G. P. Van Der Laan and A. A. C. M. Beenackers, *Catal. Rev.*, 1999, **41**, 255-318.
6. H. Schulz, *Appl. Catal. A*, 1999, **186**, 3-12.
7. C. Marcilly, *Acido-basic Catalysis*, Technip, Paris, 2005.
8. J. P. Franck, in *Fundamental and industrial aspects of catalysis by metals*, eds. B. Imelik, G. A. Martin and A. J. Renouprez, Editions du CNRS, Paris, 1984, p. 412.
9. J. H. Sinfelt, in *Handbook of Heterogeneous Catalysis*, eds. G. Ertl, E. Knözinger and J. Weitkamp, Wiley, Weinheim, 1997, pp. 1939-1955.
10. R. J. Farrauto and R. M. Heck, *Catal. Today*, 1999, **51**, 351-360.
11. J. Kašpar, P. Fornasiero and N. Hickey, *Catal. Today*, 2003, **77**, 419-449.

12. R. Burch, *Catal. Rev.*, 2004, **46**, 271-334.
13. S. Roy and A. Baiker, *Chem. Rev.*, 2009, **109**, 4054-4091.
14. P. Granger and V. I. Parvulescu, *Chem. Rev.*, 2011, **111**, 3155-3207.
15. P. Sabatier, *La Catalyse en Chimie Organique*, C. Beranger, Paris, 1913.
16. I. Langmuir, *Chem. Rev.*, 1930, **6**, 451-479.
17. G. Ertl, *Angew. Chem. Int. Ed.*, 2008, **47**, 3524-3535.
18. A. C. Byrns, W. E. Bradley and M. W. Lee, *Ind. Eng. Chem.*, 1943, **35**, 1160-1167.
19. O. Weisser and S. Landa, *Sulphide catalysts: their properties and applications*, Pergamon Press, 1973.
20. P. Raybaud, C. Chizallet, C. Mager-Maury, M. Digne, H. Toulhoat and P. Sautet, *J. Catal.*, 2013, **308**, 328-340.
21. F. Schüth, O. Busch, C. Hoffmann, T. Johann, C. Kiener, D. Demuth, J. Klein, S. Schunk, W. Strehlau and T. Zech, *Topics Catal.*, 2002, **21**, 55-66.
22. K. Jähnisch, V. Hessel, H. Löwe and M. Baerns, *Angew. Chem. Int. Ed.*, 2004, **43**, 406-446.
23. C. Mirodatos, *Oil Gas Sci. Technol. - Rev. IFP*, 2013, **68**, 403-413.
24. G. Ertl and H.-J. Freund, *Physics Today*, 1999, **52**, 32-38.
25. C. R. Henry, *Surf. Sci. Rep.*, 1998, **31**, 231-325.
26. F. Zaera, *Prog. Surf. Sci.*, 2001, **69**, 1-98.
27. H.-J. Freund, *Surf. Sci.*, 2002, **500**, 271-299.
28. H. J. Freund, *Chem. Eur. J.*, 2010, **16**, 9384-9397.
29. G. A. Somorjai, H. Frei and J. Y. Park, *J. Am. Chem. Soc.*, 2009, **131**, 16589-16605.
30. F. Meunier, *ACS Nano*, 2008, **2**, 2441-2444.
31. H. Friedrich, P. E. de Jongh, A. J. Verkleij and K. P. de Jong, *Chem. Rev.*, 2009, **109**, 1613-1629.
32. B. M. Weckhuysen, *Angew. Chem. Int. Ed.*, 2009, **48**, 4910-4943.
33. S. Bordiga, E. Groppo, G. Agostini, J. A. van Bokhoven and C. Lamberti, *Chem. Rev.*, 2013, **113**, 1736-1850.
34. I. L. Buurmans and B. M. Weckhuysen, *Nature Chem.*, 2012, **4**, 873-886.
35. A. Brückner, *Catal. Rev.*, 2003, **45**, 97-150.
36. M. A. Bãñares, *Catal. Today*, 2005, **100**, 71-77.
37. J. T. Gleaves, G. S. Yablonskii, P. Phanawadee and Y. Schuurman, *Appl. Catal. A*, 1997, **160**, 55-88.
38. J. Schweicher, A. Bundhoo, A. Frennet, N. Kruse, H. Daly and F. C. Meunier, *J. Phys. Chem. C*, 2010, **114**, 2248-2255.
39. A. T. Bell, *Science*, 2003, **299**, 1688-1691.
40. P. Hohenberg and W. Kohn, *Phys. Rev.*, 1964, **136**, B864-B871.
41. R. A. van Santen and M. Neurock, *Molecular Heterogeneous Catalysis*, Wiley-VCH, Weinheim, 2006.
42. R. A. van Santen and P. Sautet, *Computational Methods in Catalysis and Materials Science*, Wiley-VCH, Weinheim, 2009.
43. M. K. Sabbe, M.-F. Reyniers and K. Reuter, *Catal. Sci. Technol.*, 2012, **2**, 2010-2024.
44. N. Lopez, N. Almora-Barrios, G. Carchini, P. Blonski, L. Bellarosa, R. Garcia-Muelas, G. Novell-Leruth and M. Garcia-Mota, *Catal. Sci. Technol.*, 2012, **2**, 2405-2417.
45. A. Warshel and M. Levitt, *J. Mol. Biol.*, 1976, **103**, 227-249.
46. J. Sauer and M. Sierka, *J. Comput. Chem.*, 2000, **21**, 1470-1493.
47. P. V. Sushko, J. L. Gavartin and A. L. Shluger, *J. Phys. Chem. B*, 2002, **106**, 2269-2276.
48. J. Hafner, L. Benco and T. Bucko, *Topics Catal.*, 2006, **37**, 41-54.

49. B. Hammer and J. K. Nørskov, *Adv. Catal.*, 2000, **45**, 71-129.
50. J. K. Nørskov, T. Bligaard, J. Rossmeisl and C. H. Christensen, *Nature Chem.*, 2009, **1**, 37-46.
51. R. van Santen, *Acc. Chem. Res.*, 2009, **42**, 57-66.
52. M. Che and A. J. Tench, *Adv. Catal.*, 1982, **31**, 77-133.
53. M. L. Bailly, C. Chizallet, G. Costentin, J. M. Krafft, H. Lauron-Pernot and M. Che, *J. Catal.*, 2005, **235**, 413-422.
54. C. Chizallet, S. Lazare, D. Bazer-Bachi, F. Bonnier, V. Lecocq, E. Soyer, A. A. Quoineaud and N. Bats, *J. Am. Chem. Soc.*, 2010, **132**, 12365-12377.
55. M. Behrens, F. Studt, I. Kasatkin, S. Kühl, M. Häveker, F. Abild-Pedersen, S. Zander, F. Girgsdies, P. Kurr, B. J. Kniep, M. Tovar, R. W. Fischer, J. K. Nørskov and R. Schlögl, *Science*, 2012, **336**, 893-897.
56. O. Cairon, T. Chevreau and J. C. Lavalley, *J. Chem. Soc., Faraday Trans.*, 1998, **94**, 3039-3047.
57. J. To, A. A. Sokol, S. A. French, C. R. A. Catlow, P. Sherwood and H. J. J. van Dam, *Angew. Chem. Int. Ed.*, 2006, **45**, 1633-1638.
58. S. Polarz, J. Strunk, V. Ischenko, M. W. E. van den Berg, O. Hinrichsen, M. Muhler and M. Driess, *Angew. Chem. Int. Ed.*, 2006, **45**, 2965-2969.
59. S. A. French, A. A. Sokol, S. T. Bromley, C. R. A. Catlow, S. C. Rogers, F. King and P. Sherwood, *Angew. Chem., Int. Ed.*, 2001, **40**, 4437.
60. C. Wöll, *Prog. Surf. Sci.*, 2007, **82**, 55-120.
61. F. Esch, S. Fabris, L. Zhou, T. Montini, C. Africh, P. Fornasiero, G. Comelli and R. Rosei, *Science*, 2005, **309**, 752-755.
62. C. Drouilly, J. M. Krafft, F. Averseng, H. Lauron-Pernot, D. Bazer-Bachi, C. Chizallet, V. Lecocq and G. Costentin, *Appl. Catal. A*, 2013, **453**, 121-129.
63. M. Breyse, P. Afanasiev, C. Geantet and M. Vrinat, *Catal. Today*, 2003, **86**, 5-16.
64. B. M. Weckhuysen and D. E. Keller, *Catal. Today*, 2003, **78**, 25-46.
65. M. Comotti, W.-C. Li, B. Spliethoff and F. Schüth, *J. Am. Chem. Soc.*, 2005, **128**, 917-924.
66. C. Bouchy, G. Hastoy, E. Guillon and J. A. Martens, *Oil Gas Sci. Technol. - Rev. IFP*, 2009, **64**, 91-112.
67. K. Reuter and M. Scheffler, *Phys. Rev. Lett.*, 2003, **90**.
68. J. Rogal, K. Reuter and M. Scheffler, *Phys. Rev. Lett.*, 2007, **98**.
69. D. Teschner, J. Borsodi, A. Woosch, Z. Révay, M. Hävecker, A. Knop-Gericke, S. D. K. Jackson and R. Schlögl, *Science*, 2008, **320**, 86-89.
70. D. Teschner, Z. Révay, J. Borsodi, M. Hävecker, A. Knop-Gericke, R. Schlögl, D. Milroy, S. D. Jackson, D. Torres and P. Sautet, *Angew. Chem., Int. Ed.*, 2008, **47**, 9274-9278.
71. M. Armbrüster, M. Behrens, F. Cinquini, K. Föttinger, Y. Grin, A. Haghofner, B. Klötzer, A. Knop-Gericke, H. Lorenz, A. Ota, S. Penner, J. Prinz, C. Rameshan, Z. Révay, D. Rosenthal, G. Rupprechter, P. Sautet, R. Schlögl, L. Shao, L. Szentmiklósi, D. Teschner, D. Torres, R. Wagner, R. Widmer and G. Wowsnick, *ChemCatChem*, 2012, **4**, 1048-1063.
72. I. M. Ciobîcă, R. A. van Santen, P. J. van Berge and J. van de Loosdrecht, *Surf. Sci.*, 2008, **602**, 17-27.
73. M. Digne, P. Sautet, P. Raybaud, P. Euzen and H. Toulhoat, *J. Catal.*, 2002, **211**, 1-5.
74. M. Digne, P. Sautet, P. Raybaud, P. Euzen and H. Toulhoat, *J. Catal.*, 2004, **226**, 54-68.
75. C. Chizallet, G. Costentin, M. Che, F. Delbecq and P. Sautet, *J. Phys. Chem. B*, 2006, **110**, 15878-15886.

76. S. T. Korhonen, M. Calatayud and A. O. Krause, *J. Phys. Chem. C*, 2008, **112**, 6469-6476.
77. C. Arrouvel, M. Digne, M. Breysse, H. Toulhoat and P. Raybaud, *J. Catal.*, 2004, **222**, 152-166.
78. C. Chizallet, M. Digne, C. Arrouvel, P. Raybaud, F. Delbecq, G. Costentin, M. Che, P. Sautet and H. Toulhoat, *Topics Catal.*, 2009, **52**, 1005-1016.
79. J. Weitkamp, *ChemCatChem*, 2012, **4**, 292-306.
80. G. W. Huber, R. D. Cortright and J. A. Dumesic, *Angew. Chem. Int. Ed.*, 2004, **43**, 1549-1551.
81. J. Q. Bond, D. M. Alonso, D. Wang, R. W. West and J. A. Dumesic, *Science*, 2010, **327**, 1110-1114.
82. G. Kresse and J. Hafner, *Phys. Rev. B*, 1994, **49**, 14251-14269.
83. G. Kresse and J. Furthmüller, *Phys. Rev. B*, 1996, **54**, 11169:11161-11118.
84. J. Perdew and Y. Wang, *Phys. Rev. B*, 1992, **45**, 13244-13249.
85. J. Perdew, K. Burke and M. Ernzerhof, *Phys. Rev. Lett.*, 1996, **77**, 3865-3868.
86. G. Kresse and D. Joubert, *Phys. Rev. B*, 1999, **59**, 1758-1775.
87. C. Chizallet and P. Raybaud, *Angew. Chem. Int. Ed.*, 2009, **48**, 2891-2893.
88. C. Mager-Maury, G. Bonnard, C. Chizallet, P. Sautet and P. Raybaud, *ChemCatChem*, 2011, **3**, 200-207.
89. X. Krokidis, P. Raybaud, A. E. Gobichon, B. Rebours, P. Euzen and H. Toulhoat, *J. Phys. Chem. B*, 2001, **105**, 5121-5130.
90. M. Digne, P. Raybaud, P. Sautet, D. Guillaume and H. Toulhoat, *J. Am. Chem. Soc.*, 2008, **130**, 11030-11039.
91. J. Sauer, *Chem. Rev.*, 1989, **89**, 199-255.
92. R. van Santen and G. J. Kramer, *Chem. Rev.*, 1995, **95**, 637-660.
93. W. E. Farneth and R. J. Gorte, *Chem. Rev.*, 1995, **95**, 615-635.
94. G. Busca, *Chem. Rev.*, 2007, **107**, 5366-5410.
95. F. Bertoncini, A. Bonduelle-Skrzypcak, J. Francis and E. Guillon, in *Catalysis by transition metal sulphides: from molecular theory to industrial applications*, eds. H. Toulhoat and P. Raybaud, Technip, 2013, pp. 609-677.
96. M. Trombetta, G. Busca, S. Rossini, V. Piccoli, U. Cornaro, A. Guercio, R. Catani and R. J. Willey, *J. Catal.*, 1998, **179**, 581-596.
97. W. Daniell, U. Schubert, R. Glöckler, A. Meyer, K. Noweck and H. Knözinger, *Appl. Catal. A*, 2000, **196**, 247-260.
98. G. Crépeau, V. Montouillout, A. Vimont, L. Mariey, T. Cseri and F. Maugé, *J. Phys. Chem. B*, 2006, **110**, 15172-15185.
99. D. G. Poduval, J. A. R. van Veen, M. S. Rigutto and E. J. M. Hensen, *Chem. Commun.*, 2010, **46**, 3466-3468.
100. M. F. Williams, B. Fonfé, C. Sievers, A. Abraham, J. A. van Bokhoven, A. Jentys, J. A. R. van Veen and J. A. Lercher, *J. Catal.*, 2007, **251**, 485-496.
101. K. Gora-Marek, M. Derewinski, P. Sarv and J. Datka, *Catal. Today*, 2005, **101**, 131-138.
102. C. Chizallet and P. Raybaud, *ChemPhysChem*, 2010, **11**, 105-108.
103. F. Leydier, C. Chizallet, A. Chaumonnot, M. Digne, E. Soyer, A. A. Quoineaud, D. Costa and P. Raybaud, *J. Catal.*, 2011, **284**, 215-229.
104. F. Leydier, C. Chizallet, D. Costa and P. Raybaud, *Chem. Commun.*, 2012, **48**, 4076-4078.
105. A. Winkler, J. Horbach, W. Kob and K. Binder, *J. Chem. Phys.*, 2004, **120**, 384-393.
106. M. Benoit, S. Ispas and M. Tuckerman, *Phys. Rev. B*, 2001, **64**, 224205.

107. R. Duchateau, R. J. Harmsen, H. C. L. Abbenhuis, R. van Santen, A. Meetsma, S. K. H. Thiele and M. Kranenburg, *Chem. Eur. J.*, 1999, **5**, 3130-3135.
108. A. W. Moses, N. A. Ramsahye, C. Raab, H. D. Leifeste, S. Chattopadhyay, B. F. Chmelka, J. Eckert and S. L. Scott, *Organometallics*, 2006, **25**, 2157-2165.
109. A. Chaumonnot, in *Catalysis by transition metal sulphides: from molecular theory to industrial applications*, eds. H. Toulhoat and P. Raybaud, Technip, 2013, pp. 225-243.
110. N. Katada and M. Niwa, *Chem. Vap. Deposition*, 1996, **2**, 125-134.
111. J. D. Alexander, A. N. Gent and P. N. Henriksen, *J. Chem. Phys.*, 1985, **83**, 5981-5987.
112. M. Lindblad and A. Root, *Stud. Surf. Sci. Catal.*, 1998, **118**, 817-826.
113. P. Sarrazin, S. Kasztelan, N. Zanier-Szydłowski, J. P. Bonnelle and J. Grimblot, *J. Phys. Chem.*, 1993, **97**, 5947-5953.
114. B. M. De Witte, P. J. Grobet and J. B. Uytterhoeven, *J. Phys. Chem.*, 1995, **99**, 6961-6965.
115. J. P. Gilson, G. C. Edwards, A. W. Peters, K. Rajagopalan, R. F. Wormsbecher, T. G. Roberie and M. P. Shatlock, *J. Chem. Soc., Chem. Commun.*, 1987, 91-92.
116. M. Caillot, A. Chaumonnot, M. Digne and J. A. V. Bokhoven, *ChemCatChem*, 2013, **5**, 3644-3656.
117. F. Tielens, C. Gervais, J. F. Lambert, F. Mauri and D. Costa, *Chem. Mater.*, 2008, **20**, 3336-3344.
118. K. Gora-Marek and J. Datka, *Appl. Catal. A*, 2006, **302**, 104-109.
119. B. Xu, C. Sievers, J. A. Lercher, J. A. R. van Veen, P. Giltay, R. Prins and J. A. van Bokhoven, *J. Phys. Chem. C*, 2007, **111**, 12075-12079.
120. E. J. M. Hensen, D. G. Poduval, V. Degirmenci, D. A. J. M. Ligthart, W. Chen, F. Maugé, M. S. Rigutto and J. A. R. van Veen, *J. Phys. Chem. C*, 2012, **116**, 21416-21429.
121. E. Garrone, B. Onida, B. Bonelli, C. Busco and P. Ugliengo, *J. Phys. Chem. B*, 2006, **110**, 19087-19092.
122. H. Knözinger, in *Handbook of Heterogeneous Catalysis*, eds. G. Ertl, H. Knözinger and J. Weitkamp, Wiley, Weinheim, 1997, vol. 2, pp. 707-732.
123. A. Corma, *Chem. Rev.*, 1995, **95**, 559-614.
124. J. A. Lercher, C. Gründling and G. Eder-Mirth, *Catal. Today*, 1996, **27**, 353-376.
125. A. Zecchina, C. Lamberti and S. Bordiga, *Catal. Today*, 1998, **41**, 169-177.
126. O. Cairon, *Phys. Chem. Chem. Phys.*, 2010, **12**, 6333-6336.
127. S. Vajda, M. J. Pellin, J. P. Greeley, C. L. Marshall, L. A. Curtiss, G. E. Ballentine, J. M. Elam, S. Catillon-Mucherie, P. C. Redfern, F. Mehmood and P. Zapol, *Nat. Mater.*, 2009, **8**, 213-216.
128. P. Euzen, P. Raybaud, X. Krokidis, H. Toulhoat, J. L. Loarer, J.-P. Jolivet and C. Froidefond, in *Handbook of Porous Solids*, eds. F. Schüth, K. S. W. Sing and J. Weitkamp, Wiley-VCH, Weinheim, 2002.
129. P. D. Nellist and S. J. Pennycook, *Science*, 1996, **274**, 413-415.
130. Y. Ji, A. M. J. van der Eerden, V. Koot, P. J. Kooyman, J. D. Meeldijk, B. M. Weckhuysen and D. C. Koningsberger, *J. Catal.*, 2005, **234**, 376-384.
131. J. H. Kwak, J. Hu, D. Mei, C. W. Yi, D. H. Kim, C. H. F. Peden, L. F. Allard and J. Szanyi, *Science*, 2009, **325**, 1670-1673.
132. S. Bradley, W. Sinkler, D. Blom, W. Bigelow, P. Voyles and L. Allard, *Catal. Lett.*, 2012, **142**, 176-182.
133. M. W. Small, S. I. Sanchez, N. S. Marinkovic, A. I. Frenkel and R. G. Nuzzo, *ACS Nano*, 2012, **6**, 5583-5595.
134. A. K. Santra and D. W. Goodman, *J. Phys.: Condens. Matter*, 2002, **14**, R31-R62.

135. M. Sterrer, T. Risse, L. Giordano, M. Heyde, N. Nuius, H. P. Rust, G. Pacchioni and H.-J. Freund, *Angew. Chem. Int. Ed.*, 2007, **46**, 8703-8706.
136. J. H. Sinfelt, G. H. Via and F. W. Lytle, *J. Chem. Phys.*, 1978, **68**, 2009-2010.
137. J. Lynch, *Oil Gas Sci. Technol. - Rev. IFP*, 2002, **57**, 281-305.
138. M. K. Oudenhuijzen, J. A. van Bokhoven, J. T. Miller, D. E. Ramaker and D. C. Koningsberger, *J. Am. Chem. Soc.*, 2005, **127**, 1530-1540.
139. F. Behafarid, L. K. Ono, S. Mostafa, J. R. Croy, G. Shafai, S. Hong, T. S. Rahman, S. R. Bare and B. Roldan Cuenya, *Phys. Chem. Chem. Phys.*, 2012, **14**, 11766-11779.
140. H. Mistry, F. Behafarid, S. R. Bare and B. Roldan Cuenya, *ChemCatChem*, 2014, **6**, 348-352.
141. C. Verdozzi, D. R. Jennison, P. A. Schultz and M. P. Sears, *Phys. Rev. Lett.*, 1999, **82**, 799-802.
142. V. A. Nasluzov, V. V. Rivanenkov, A. M. Shor, K. M. Neyman and N. Rösch, *Chem. Phys. Lett.*, 2003, **374**, 487-495.
143. V. V. Rivanenkov, V. A. Nasluzov, A. M. Shor, K. M. Neyman and N. Rösch, *Surf. Sci.*, 2003, **525**, 173-183.
144. B. Hinnemann and E. A. Carter, *J. Phys. Chem. C*, 2007, **111**, 7105-7126.
145. C. Zhou, J. Wu, T. J. D. Kumar, N. Balakrishnan, R. C. Forrey and H. Cheng, *J. Phys. Chem. C*, 2007, **111**, 13786-13793.
146. L. G. V. Briquet, C. R. A. Catlow and S. A. French, *J. Phys. Chem. C*, 2008, **112**, 18948-18954.
147. L. G. V. Briquet, C. R. A. Catlow and S. A. French, *J. Phys. Chem. C*, 2009, **113**, 16747-16756.
148. L. Xiao and W. F. Schneider, *Surf. Sci.*, 2008, **602**, 3445.
149. N. A. Deskins, D. Mei and M. Dupuis, *Surf. Sci.*, 2009, **603**, 2793-2807.
150. F. Vila, J. J. Rehr, J. Kas, R. G. Nuzzo and A. I. Frenkel, *Phys. Rev. B*, 2008, **78**, 121404:121401-121404.
151. F. Ahmed, M. K. Alam, A. Suzuki, M. Koyama, H. Tsuboi, N. Hatakeyama, A. Endou, H. Takaba, C. A. Del Carpio, M. Kubo and A. Miyamoto, *J. Phys. Chem. C*, 2009, **113**, 15676-15683.
152. A. Jahel, V. Moizan-Baslé, C. Chizallet, P. Raybaud, J. Olivier-Fourcade, J. C. Jumas, P. Avenier and S. Lacombe, *J. Phys. Chem. C*, 2012, **116**, 10073-10083.
153. F. D. Vila, J. J. Rehr, S. D. Kelly and S. R. Bare, *J. Phys. Chem. C*, 2013, **117**, 12446-12457.
154. C. H. Hu, C. Chizallet, C. Mager-Maury, M. Corral Valero, P. Sautet, H. Toulhoat and P. Raybaud, *J. Catal.*, 2010, **274**, 99-110.
155. C. Mager-Maury, C. Chizallet, P. Sautet and P. Raybaud, *ACS Catalysis*, 2012, **2**, 1346-1357.
156. C. H. Hu, C. Chizallet, H. Toulhoat and P. Raybaud, *Phys. Rev. B*, 2009, **79**, 195416:195411-195411.
157. J. Berdala, E. Freund and J. Lynch, *Journal de Physique*, 1986, **47**, 269-272.
158. D. J. O'Rear, D. G. Löffler and M. Boudart, *J. Catal.*, 1990, **121**, 131-140.
159. B. J. Kip, F. B. M. Duivenvoorden, D. C. Koningsberger and R. Prins, *J. Catal.*, 1987, **105**, 26-38.
160. P. Ferreira-Aparicio, A. Guerrero-Ruiz and I. Rodriguez-Ramos, *J. Chem. Soc., Faraday Trans.*, 1997, **93**, 3563-3567.
161. J. T. Miller, B. L. Meyers, F. S. Modica, G. S. Lane, M. Vaarkamp and D. C. Koningsberger, *J. Catal.*, 1993, **143**, 395-408.
162. E. Bus, J. T. Miller, A. J. Kropf, R. Prins and J. A. van Bokhoven, *Phys. Chem. Chem. Phys.*, 2006, **8**, 3248-3258.

163. S. I. Sanchez, L. D. Menard, A. Bram, J. H. Kang, M. W. Small, R. G. Nuzzo and A. I. Frenkel, *J. Am. Chem. Soc.*, 2009, **131**, 7040-7054.
164. J. Singh, R. C. Nelson, B. C. Vicente, S. L. Scott and J. A. van Bokhoven, *Phys. Chem. Chem. Phys.*, 2010, **12**, 5668-5677.
165. P. Raybaud, C. Chizallet, H. Toulhoat and P. Sautet, *Phys. Chem. Chem. Phys.*, 2012, **14**, 16773-16774.
166. G. C. Bond and R. H. Cunningham, *J. Catal.*, 1997, **166**, 172-185.
167. G. C. Bond, *Catal. Today*, 1999, **49**, 41-48.
168. C. Chizallet, G. Bonnard, E. Krebs, L. Bisson, C. Thomazeau and P. Raybaud, *J. Phys. Chem. C*, 2011, **115**, 12135-12149.
169. E. Benazzi, L. Leite, N. Marchal-George, H. Toulhoat and P. Raybaud, *J. Catal.*, 2003, **217**, 376-387.
170. H. Toulhoat, P. Raybaud and E. Benazzi, *J. Catal.*, 2004, **221**, 500-509.
171. S. Pega, C. Boissière, D. Grosso, T. Azaïs, A. Chaumonnot and C. Sanchez, *Angew. Chem. Int. Ed.*, 2009, **48**, 2784-2787.
172. M.-C. Silaghi, C. Chizallet and P. Raybaud, *Mic. Mes. Mat.*, 2014, **191**, 82-96.
173. J. A. Martens, G. Vanbutsele, P. A. Jacobs, J. Denayer, R. Ocaoglu, G. Baron, J. A. Muñoz Arroyo, J. Thybaut and G. B. Marin, *Catal. Today*, 2001, **65**, 111-116.
174. J. A. Martens, W. Souverijns, W. Verrelst, R. Parton, G. F. Froment and P. A. Jacobs, *Angew. Chem. Int. Ed.*, 1995, **34**, 2528-2530.
175. W. A. de Jong, E. Bylaska, N. Govind, C. L. Janssen, K. Kowalski, T. Muller, I. M. B. Nielsen, H. J. J. van Dam, V. Veryazov and R. Lindh, *Phys. Chem. Chem. Phys.*, 2010, **12**, 6896-6920.
176. J. K. Nørskov, T. Bligaard, A. Logadottir, S. Bahn, L. B. Hansen, M. Bollinger, H. Bengaard, B. Hammer, Z. Sljivancanin, M. Mavrikakis, Y. Xu, S. Dahl and C. J. H. Jacobsen, *J. Catal.*, 2002, **209**, 275-278.
177. H. Toulhoat and P. Raybaud, *J. Catal.*, 2003, **216**, 63-72.
178. R. van Santen, M. Neurock and S. G. Shetty, *Chem. Rev.*, 2010, **110**, 2005-2048.
179. J. K. Nørskov and T. Bligaard, *Angew. Chem. Int. Ed.*, 2013, **52**, 776-777.
180. F. Corvaisier, Y. Schuurman, A. Fecant, C. Thomazeau, P. Raybaud, H. Toulhoat and D. Farrusseng, *J. Catal.*, 2013, **307**, 352-361.
181. E. J. Ras, M. J. Louwse, M. C. Mittelmeijer-Hazeleger and G. Rothenberg, *Phys. Chem. Chem. Phys.*, 2013, **15**, 4436-4443.
182. E. Johnson, *Science*, 2002, **296**, 477-478.
183. M.-P. Gaigeot, M. Sprik and M. Sulpizi, *J. Phys.: Condens. Matter*, 2012, **24**, 124106.
184. J. Carrasco, A. Hodgson and A. Michaelides, *Nat Mater*, 2012, **11**, 667-674.
185. F. Zaera, *Chem. Rev.*, 2012, **112**, 2920-2986.
186. S. Laref, Y. Li, M.-L. Bocquet, F. Delbecq, P. Sautet and D. Loffreda, *Phys. Chem. Chem. Phys.*, 2011, **13**, 11827-11837.
187. B. N. Zope, D. D. Hibbits, M. Neurock and R. J. Davis, *Science*, 2010, **330**, 74.
188. A. C. T. van Duin, S. Dasgupta, F. Lorant and W. A. Goddard, *J. Phys. Chem. A*, 2001, **105**, 9396-9409.
189. S. Matera and K. Reuter, *Catal. Lett.*, 2009, **133**, 156-159.
190. D. G. Vlachos, *AIChE J.*, 2012, **58**, 1314-1325.
191. N. Rankovic, C. Chizallet, A. Nicolle, D. Berthout and P. Da Costa, *Oil Gas Sci. Technol. - Rev. IFP*, 2013, **68**, 995-1005.
192. R. F. de Moraes, P. Sautet, D. Loffreda and A. A. Franco, *Electrochim. Acta*, 2011, **56**, 10842-10856.
193. M. Saliccioli, M. Stamatakis, S. Caratzoulas and D. G. Vlachos, *Chem. Eng. Sci.*, 2011, **66**, 4319-4355.

194. M. Maestri and K. Reuter, *Chem. Eng. Sci.*, 2012, **74**, 296-299.
195. N. Rankovic, C. Chizallet, A. Nicolle and P. Da Costa, *Ind. Eng. Chem. Res.*, 2013, **52**, 9086-9098.